

How Fast Can Cracks Propagate?

Farid F. Abraham¹ and Huajian Gao²

¹*IBM Research Division, Almaden Research Center, San Jose, California 95120*

²*Division of Mechanics and Computation, Department of Mechanical Engineering, Stanford University, Stanford, California 94305*
(Received 8 June 1999)

We have performed atomic simulations of crack propagation along a weak interface joining two harmonic crystals. The simulations show that a mode II shear dominated crack can accelerate to the Rayleigh wave speed and then nucleate an intersonic daughter that travels at the longitudinal wave speed. This contradicts the general belief that a crack can travel no faster than the Rayleigh speed.

PACS numbers: 62.20.Mk, 61.20.Ja, 61.72.Bb, 68.35.Bs

An important issue in rapid brittle fracture is the limiting speed of crack propagation [1]. It is widely believed that a brittle crack cannot propagate faster than the Rayleigh wave speed. The origin for this belief stems from the predictions of continuum mechanics [1–3]. For mode I tensile loading, theory predicts that the “forbidden velocity zone” for crack propagation is for any speed greater than the Rayleigh wave speed. For mode II shear loading, the forbidden velocity zone exists only for speeds between the Rayleigh and shear wave speeds. Hence, a mode I crack’s limiting speed is the Rayleigh speed. However, a mode II crack’s limiting speed is also the Rayleigh speed because its forbidden velocity zone between the Rayleigh and shear wave speeds acts as an impenetrable barrier for the shear crack to go beyond the Rayleigh wave speed.

Burridge [4] studied cracks growing self-similarly at the Rayleigh speed and discovered that, under mode II conditions, a positive peak of shear stress develops at a distance ahead of the tip. In comparison, no such peak exists under mode I conditions. Andrews [5] concluded that a subsonic shear crack could indeed induce microcracks moving at speeds faster than the shear wave speed. More recently, a continuum analysis of intersonic crack propagation based on a cohesive surface model was studied by Needleman [6] and showed transonic crack propagation. Analysis of the 1979 Imperial Valley earthquake [7] provided indirect observations of shear rupture in excess of the shear wave speed.

The first direct experimental observation of cracks faster than the wave speed c_t has now been reported by Rosakis *et al.* [8]. They investigated shear dominated crack growth along weak planes in a brittle polyester resin under far field asymmetrical loading. The late arrival of an experiment on intersonic fracture is due, in part, to the fact that a crack in elastic homogeneous and isotropic solids always kinks or branches out, deviating from the initial crack plane and having a zigzag crack path, once the crack tip velocity exceeds only $\sim(0.3-0.4)c_t$ [1,9,10]. In fact, the only possibility of attaining intersonic propagation is to introduce a weak path (a layer of lower toughness) so that crack growth is confined to this path, as done by Rosakis *et al.* [8]. The question of whether a transonic crack has been accelerated

from a subsonic crack or is nucleated directly as an intersonic crack has not been resolved by experiments.

To understand this phenomenon, we have performed two-dimensional molecular dynamics (MD) simulations [11] of crack propagation along a weak interface joining two harmonic crystals. The MD technique has provided valuable insights on the dynamics of dislocations [12]. Similar to cracks, a forbidden velocity zone exists for dislocations and lies between the Rayleigh and shear wave speeds [13,14]. However, Hoover and colleagues [15] reported dislocations traveling transonically at nine-tenths the longitudinal sound speed. This was also observed in simulations of fracture [10] and indentation [16].

We assume that the interatomic forces are harmonic, except for those pairs of atoms with a separation cutting the horizontal center line of the simulation slab. For these pairs, the interatomic potential is taken to be Lennard-Jones (LJ) 12:6. We express the results in terms of reduced units: lengths are scaled by the parameter σ , the value of the interatomic separation for which the LJ potential is zero, and energies are scaled by the parameter ϵ , the depth of the minimum of the LJ potential. We adopt the LJ spring constant and nearest-neighbor interactions for the harmonic lattice. The LJ potential cutoff is taken to be 2.5. Atoms along the crack line with LJ interactions bond only with their original nearest neighbors. The longitudinal wave speed c_ℓ at zero temperature and pressure is 9, and the shear wave speed $c_t = c_\ell/\sqrt{3} \approx 5.20$. The Rayleigh wave speed $c_R \approx 4.83$ is approximately 0.93 of the shear wave speed.

Our system is a 2D rectangular slab of atoms with $N_x = 1424$ atoms along the horizontal length defining the x direction and with $N_y = 712$ atoms along the vertical length defining the y direction. A horizontal slit of 200 atom distance is cut midway along the left-hand vertical slab boundary. The 2D crystal has a triangular lattice with the slit parallel to the close packed direction along which atomic spacing is equal to the lattice constant $2^{1/6}$. The initial temperature is set to be zero, and the simulation is conducted at constant energy. To study a shear dominated crack, strain rates $\dot{\epsilon}_y = 0.00005$ and $\dot{\epsilon}_x = 0.00025$ are imposed on the outermost rows of atoms defining the op-

posing horizontal faces of our two-dimensional slab. The top of the slab moves up and to the left (or in the positive y and negative x directions) and the bottom of the slab moves down and to the right (or in the negative y and positive x directions). Linear velocity gradients are established across the slab, and an increasing strain occurs in the solid slab. This leads to eventual failure of the material at the slit tip. The applied strain rates remain constant during the simulation, and the simulation is continued until the growing crack has traversed the total length of the slab. We also conducted simulations of a mode I crack with the same geometrical setup, where only an opening strain rate $\dot{\epsilon}_y = 0.00005$ is imposed. The results are discussed below.

The histories of crack velocity under mode I and mode II loading are presented in Fig. 1. The triangles show representative positions of the crack under tensile (mode I) loading as a function of time. The mode I crack quickly approaches a constant velocity, as indicated by the tip positions falling on a straight line with a slope of 4.83 equal to the reduced Rayleigh wave speed of the harmonic crystal. The mode I case shows that the crack velocity is indeed limited by the Rayleigh wave speed, consistent with the classical theories of fracture. In comparison, the dots show representative recorded positions of the crack under shear dominated (mode II) loading as a function of time. The mode II crack quickly approaches a constant velocity. After propagating at this constant velocity for a short while, the crack tip jumps to a higher constant velocity, as indicated by the positions falling on two straight lines. The slope of the first straight line is calculated to be 4.82, or the Rayleigh wave speed of the harmonic solid. The slope of the second straight line is calculated to be

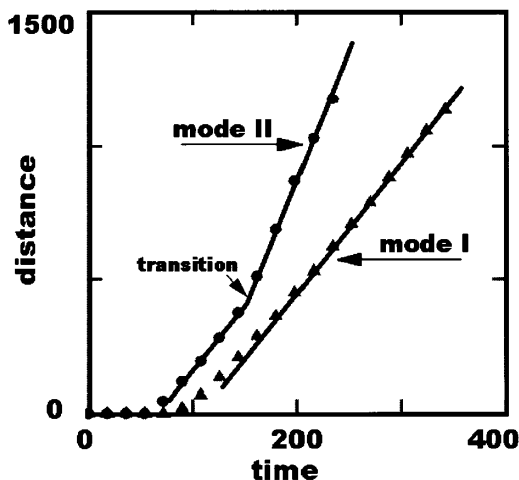


FIG. 1. The history of crack velocity under mode I and mode II loading. Note that the mode I crack is quickly accelerated to the Rayleigh wave speed and is limited by this speed. The mode II crack first accelerates to the Rayleigh wave speed, propagates at the Rayleigh speed for a while, and then jumps to the longitudinal sound speed.

8.97 which is essentially the reduced longitudinal sound speed. These results are consistent with the Mach cone angles and the expanding halo configuration shown in Fig. 2. The mode II crack thus exceeds the Rayleigh wave speed and contradicts the classical theories of fracture.

Figure 2 shows several snapshots of a mode II crack accelerating to the longitudinal sound speed. Initially, the mode II crack is subsonic with no shock waves emanating from the crack tip, as shown in Fig. 2(a). As the crack jumps over the forbidden velocity zone and attains the longitudinal wave speed, a pair of shock fronts are observed as a Mach cone emanating from the crack tip, as shown in Figs. 2(b) and 2(c). These shock fronts correspond to transverse sound waves generated at the moving crack. Note that the crack sits at the top of a circular halo which corresponds to longitudinal sound waves emitted from the crack tip. This configuration shows that the crack velocity is equal to the longitudinal wave speed. There is shock wave reflection at the vertical boundaries at the very late stage of the simulation, which is in the opposite direction of crack growth. The crack tip is not affected by the reflected shock waves. Since the crack travels at the

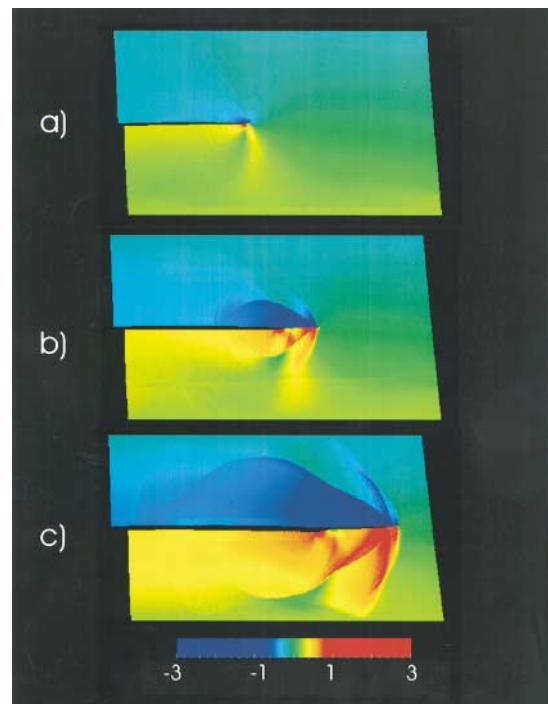


FIG. 2 (color). Transition of a subsonic crack to the longitudinal sound speed. The figures represent a progression in time from the top to the bottom. (a) A mode II shear crack travels at the Rayleigh wave speed; (b) the early-time occurrence of shock waves as the crack attains the longitudinal wave speed; (c) the late-time propagating crack traveling at the longitudinal wave speed. Note that the crack is moving at the same speed as the halo expanding at the longitudinal sound speed. The color bar shows the color map for the local atom speed in the x direction, i.e., the direction of the moving crack. The slab dimensions are approximately 800 by 1400 (in reduced units).

longitudinal wave speed, it “outruns” all of the acoustical disturbances.

The mechanism for the mode II crack “jumping” over the forbidden velocity zone is clearly shown in Fig. 3, where a series of color maps of the shear stress component σ_{xy} is used to reveal the details of this process. This transition occurs by the nucleation of an intersonic daughter crack ahead of the mother crack traveling at the Rayleigh wave speed. As the mother crack approaches the critical state of nucleation, the crack tip region is asymmetrically distorted with a bulge on the right side of the crack face, as shown in Fig. 3(a). The linear elastic solutions of dynamic crack tip field [1] predict that the opening displacements along the crack face are symmetric with respect to the crack line under mode I loading and zero under mode II loading (there is only a sliplike motion of crack surfaces under mode II). According to these solutions, the crack opening displacements should remain symmetric even under mixed mode conditions, which is inconsistent with the asymmetric distortion observed in our simulation.

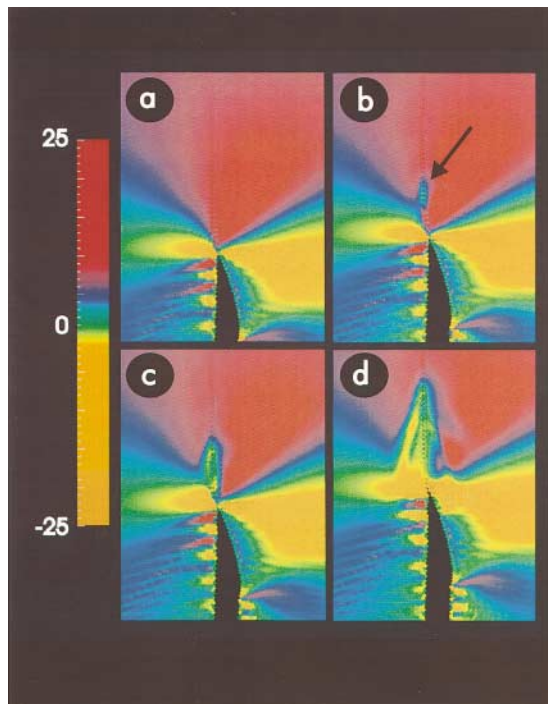


FIG. 3 (color). The nucleation of an intersonic daughter crack at the mother crack. The figures represent a progression in time from left to right and from top to bottom which are referenced as (a) to (d). (a) The approach of the critical state for the mother crack. Note the asymmetrically distorted crack tip region; (b) the birth of the intersonic crack. A very sharp slit is born ahead of the tip of the mother crack. (c)–(d) The daughter crack joins the mother crack and quickly approaches the longitudinal sound speed. The color bar shows the color map for the shear stress component σ_{xy} . The bulged mother crack is still propagating at the Rayleigh wave speed. The dimensions of the solid region shown are approximately 90 by 120 (in reduced units).

It appears that the scale of asymmetry is too large to be explained by the asymmetry of lattice. While the origin of such discrepancy between theory and simulation is not entirely clear, we believe that the crack tip distortion is a consequence of anharmonic interactions across the weak interface which causes asymmetry in the dynamical relaxation of the atoms upon bond breaking. An intuitive argument is given as follows: for the slab’s bottom half, the released atoms “snowplow” to the right into a highly compressed solid; on the slab’s top half, the released atoms move to the left into a solid that is also relaxing in the same direction into an unstrained state. The snowplowing, coupled with vertical expansion, causes local distortion of the harmonic slab on the lower side of the crack head and gives rise to the observed bulging. The shear stress distribution near the crack tip is also highly asymmetric, contradicting the mode II crack analysis of Burridge [4] and Andrews [5], although the nucleation of the daughter crack is very reminiscent of what they proposed based on continuum analysis. We observe significantly less crack opening at the tip of the daughter crack compared with that of the mother crack, indicating that the daughter crack is more dominantly mode II even though the mother crack has a mode I component. This is consistent with our observation that the mode I crack tends to be limited by the Rayleigh wave speed.

Figures 3(b)–3(d) show the detailed process of the birth of the intersonic daughter crack. It is seen that a sharp intersonic crack is nucleated at a small distance ahead of the mother crack. Color maps of atomic velocity (not shown here) show transverse Mach cones near the daughter crack. The angle of the Mach cone shows that the velocity of the daughter crack is consistent with the longitudinal wave speed. As the daughter crack moves ahead, the mother crack can still be seen as a surface bulge which trails behind at the Rayleigh wave speed. By varying the strain rates, we find that the nucleation occurs at a constant strain.

Is the intersonic daughter crack equivalent as a pair of intersonic dislocations with opposite Burgers vectors? This is an interesting question because it is now understood [16] that intersonic and supersonic velocities can be readily accessed by dislocations that are nucleated with intersonic velocities by a strong stress concentration. To answer this question, a close view of atomic positions near the daughter crack is shown in Fig. 4. This picture clearly shows that the intersonic object ahead of the mother crack is a crack with a well-defined opening and cannot be described as edge dislocations.

Our simulations demonstrate intersonic crack propagation and the existence of a “mother-daughter” crack mechanism for a subsonic shear crack to jump over the forbidden velocity zone. This mechanism is reminiscent of a similar mechanism based on continuum theories [4,5], although the continuum description cannot provide an *ab initio* description for crack formation and the details of crack tip distortion are not consistent with the continuum solutions.

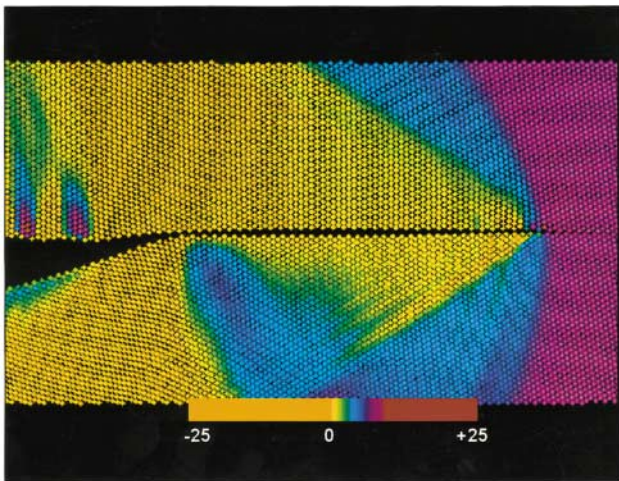


FIG. 4 (color). A close view of atomic positions near the intersonic daughter crack, which indicates that the daughter crack is a crack with a well-defined opening and cannot be regarded as a pair of edge dislocations with opposite Burgers vectors.

The birth of the daughter crack cannot be characterized by a critical energy release rate or a critical stress intensity factor near the mother crack because both of these quantities vanish at the Rayleigh wave speed. It seems that the only possible mechanism by which the daughter crack can be nucleated is by the finite stress peak ahead of the mother crack, and along the weak bonding line, as measured in the stress field and discussed by Burridge [4]. A more detailed analysis of this mechanism will be discussed in a forthcoming paper.

We have also made further extensions to this study. For example, we have set the strain rates $\dot{\epsilon}_x$ and $\dot{\epsilon}_y$ equal to zero at the time of nucleation of the intersonic crack and still observed a constant propagation velocity of the crack at the longitudinal wave speed throughout its passage to complete cleavage. However, the acoustical disturbances are much less “explosive.” If the slab is allowed to spring back by completely releasing the applied loads as soon as the daughter crack is nucleated, the crack speed drops to $\sqrt{2}c_t$ and propagates at this speed until complete cleavage occurs. This loading process seems to closely resemble the dynamic impact loading conditions in the experiments

of Rosakis *et al.* [8], and our results are entirely consistent with their corresponding experimental observations.

This paper nicely complements experimental observations of intersonic fracture [8] and provides an explanation of intersonic rupture observed for shallow crustal earthquakes [3]. Atomistic simulations yield “*ab initio*” information about crack tip formation and deformation at length scales unattainable by experimental measurement and unpredictable by continuum elasticity theory and, hence, gives additional insights into the complex mechanisms of materials failure.

F. F. A.’s interest in this problem was initiated by a conversation with Professor Young Huang at the University of Illinois. H. G. acknowledges many discussions with Professor Huang on this subject. F. F. A. acknowledges support from the USAF Wright-Patterson High Performance Computing Center and the San Diego Supercomputer Center which has its major funding from NSF. F. F. A. wishes to thank DOD’s HPCMO for financial support.

-
- [1] L. B. Freund, *Dynamical Fracture Mechanics* (Cambridge University Press, New York, 1990).
 - [2] L. B. Freund, *J. Geophys. Res.* **84**, 2199 (1979).
 - [3] K. B. Broberg, *Int. J. Fract.* **39**, 1 (1989).
 - [4] R. Burridge, *Geophys. J. R. Astron. Soc.* **35**, 439 (1973).
 - [5] D. J. Andrews, *J. Geophys. Res.* **81**, 5679 (1976).
 - [6] A. Needleman, *J. Appl. Mech.* (to be published).
 - [7] R. J. Archuleta, *Bull. Seismol. Soc. Am.* **72**, 1927 (1982).
 - [8] A. J. Rosakis, O. Samudrala, and D. Coker, *Science* **284**, 1337 (1999).
 - [9] H. Gao, *J. Mech. Phys. Solids* **41**, 457 (1993).
 - [10] F. F. Abraham, D. Brodbeck, R. Rafeey, and W. E. Rudge, *Phys. Rev. Lett.* **73**, 272 (1994); *J. Mech. Phys. Solids* **45**, 1595 (1997).
 - [11] M. P. Allen and D. J. Tildesley, *Computer Simulation of Liquids* (Clarendon Press, Oxford, 1987).
 - [12] V. Bulatov, F. F. Abraham, L. Kubin, B. Devincre, and S. Yip, *Nature (London)* **391**, 669 (1998).
 - [13] J. D. Eshelby, *Proc. Phys. Soc.* **62A**, 307 (1949).
 - [14] J. J. Weertman, *J. Appl. Phys.* **38**, 5293 (1967).
 - [15] Wm. G. Hoover, N. E. Hoover, and W. C. Moss, *Phys. Lett.* **63A**, 324 (1977).
 - [16] P. Gumbsch and H. Gao, *Science* **283**, 968 (1999).